

Max-Planck-Institut für demografische Forschung
Max Planck Institute for Demographic Research

Konrad-Zuse-Strasse 1 • D-18057 Rostock • Germany • Tel +49 (0) 3 81 20 81 - 0 • Fax +49 (0) 3 81 20 81 - 202 • www.demogr.mpg.de

MPIDR Working Paper WP 2017-007 | March 2017

A cause-of-death decomposition of the young adult mortality hump

Adrien Remund | adrien.remund@unige.ch
Carlo G. Camarda
Tim Riffe | riffe@demogr.mpg.de

This working paper has been approved for release by: Christina Bohk-Ewald (bohkewald@demogr.mpg.de),
Deputy Head of the Laboratory of Population Health.

© **Copyright is held by the authors.**

Working papers of the Max Planck Institute for Demographic Research receive only limited review. Views or opinions expressed in working papers are attributable to the authors and do not necessarily reflect those of the Institute.

A cause-of-death decomposition of the young adult mortality hump

Adrien Remund¹, Carlo G. Camarda², and Tim Riffe³

¹*Institut national d'études démographiques & University of Geneva*

²*Institut national d'études démographiques*

³*Max Planck Institute for Demographic Research*

March 16, 2017

Abstract

We propose a method to decompose the young adult mortality hump by cause of death. This method is based on a flexible shape-decomposition of mortality rates that separates cause-of-death contributions to the hump from senescent mortality. We apply the method to US males and females from 1959 to 2010. Results show divergences between time trends of hump and observed deaths, both for all-cause and cause-specific mortality. The study of the hump shape reveals age, period and cohort effects, suggesting that it is formed by a complex combination of different forces of biological and socioeconomic nature. Male and female humps share some traits in all-cause shape and trend, but also differ by their overall magnitude and cause-specific contributions. Notably, among males the contributions of traffic and other accidents were progressively replaced by those of suicides, homicides and poisonings, whereas among females traffic accidents remained the major contributor to the hump.

Correspondence

adrien.remund@unige.ch, +41.22.379.89.23

Keywords

smoothing, competing-risk model, causes of death, decomposition, young adult mortality hump, excess mortality

Acknowledgements

This study was conducted in the framework of the project "From disparities in mortality trends to future health challenges (DIMOCHA)" funded by Deutsche Forschungsgemeinschaft (DFG) (Germany) (JA 2302/1-1) and Agence nationale de la recherche (ANR) (France) (ANR-12-FRAL-0003-01). It also benefitted from an Early Postdoc.Mobility grant from the Swiss National Science Foundation. We thank the Human Mortality Database for providing us with an early release of their US cause-of-death data.

1 Introduction

Human mortality patterns usually include a brief period of excess mortality in young adult ages, often called the young adult mortality hump. Although the hump was first described long ago (Thiele, 1871), and most demographers could spontaneously draw its pattern on a napkin, recognizability has not led to extensive theoretical or analytic attention. Consequently, empirical research on the hump has been scarce. One exception is a study on its peak location (Goldstein, 2011). Aside from this, research on young adult mortality has not considered the hump pattern as a separate phenomenon from the broader mortality context. Parametric models that do separate the hump have done so for the sake of a better fit to all-cause mortality, but these have not been used to study the hump specifically. We address these shortcomings by first proposing a definition of the mortality hump, operationalized as young adult excess mortality. We then describe a flexible method of measuring the hump by age and causes of death based on a non-parametric shape-decomposition of mortality.

[Figure 1 about here.]

To decompose the shape of mortality entails treating a given mortality age-profile as a composite of a set of stylized patterns that capture specific aggregate features of the shape of mortality, and requires no assumptions about individual risk trajectories. The full age pattern of the force of mortality can be parsimoniously captured by partitioning into three primary phases that may overlap (Figure 1). The first phase, ontogenescence, consists in rapidly declining mortality from birth (Levitis, 2011). In most of adulthood, the force of mortality increases at a roughly stable relative pace (Gompertz, 1825) in a pattern known as senescence, until about age 90 when it appears to decelerate to a plateau (Horiuchi & Wilmoth, 1998; Vaupel, 1997).

Between childhood and adulthood, the force of mortality often includes what can be described as a hump. This feature is mostly visible between about 10 and 30 years of age, although it may extend further. We define the hump as a positive deviation from the steady pace of senescence. As a deviation from a Gompertz age-pattern, the hump is as much a feature of the rate of change over age as it is of an absolute age trajectory. Mortality humps of similar articulation may appear in both high and low mortality contexts. A humpless mortality curve may also have higher mortality in the same age-range as an observed hump from a lower mortality life-table. Some deaths in young adulthood ought to be attributable to a senescent process governed by the same forces shaping senescent mortality in higher ages (see area A1 in Figure 1). If we accept this possibility, then the young-adult senescent pattern may be presumed to abide by the same Gompertzian laws as older ages, leaving the hump as an identifiable excess.

We make no assumptions about particular phases within the age-patterns of individual causes of death, but we would like to know to what extent specific causes of death contribute to the all-cause hump. Causes of death contribute to different extents to the patterns observed in all-cause mortality. Crucially, some causes of death contribute to the hump and some do not. Causes of death that contribute to the hump often also contribute to senescent mortality. Cause-specific contributions to the hump may also cover slightly different age ranges, and they may shift over time. Further, strictly senescent causes of death often begin in young adult ages. This is all to say, not all causes of death in the age range of a given all-cause mortality hump contribute to the hump, and even those causes that do contribute to the hump may also only do so partially. Common age-cause decompositions of mortality differences such as those of Arriaga (1984), Pollard (1982), Andreev (1982) and Pressat (1985), as well as studies of the leading causes of death in early adulthood that use arbitrary age ranges such as 10-34 (Heuveline, 2002) or 10-24 (Blum, 2009; Patton et al., 2009), do not account for these key aspects of the hump.

We therefore propose a decomposition method that takes into account the shape of mortality, that intuitively separates the hump from the rest of mortality, and which yields a consistent decomposition by age, cause of death, and shape components. We give a formal description of the method, which follows directly from our definition of the hump as excess mortality. We follow with an application to cause of death data in the USA, comparing our decomposition method with the standard age-cause decomposition of life expectancy. Our method gives a well-suited and informative breakdown of the hump into contributions from particular ages and causes of death. Results isolate excess mortality

53 associated with the transition to adulthood, which would otherwise remain invisible, and which may
54 be useful to inform theory and policy relating to vulnerability in this phase of the lifecourse.

55 2 Methods

56 In general, excess mortality can be defined as all deaths that exceed what one would expect from a
57 reference pattern of mortality. A reference may be a mortality profile from a different time point,
58 another population, or a sub-population. The reference we use to measure the hump is that set by
59 the prevailing level of mortality as defined by the sum of all phases except the hump. In this sense,
60 our approach can be seen as a shape-based method of mortality rate decomposition operationalized
61 by defining an additive model in which the force of mortality is the sum of different components
62 corresponding to the phases described. Each of these components describes a particular simplified
63 mortality pattern that is more or less expressed during a specific period of the life course, namely
64 ontogenescence, the hump, and senescence, which can integrate a plateau at very old ages.

65 Figure 1 illustrates this additive construction and hints at the arbitrariness of setting strict age
66 bounds for the hump. In this example the total force of mortality starts increasing again around
67 age 30. Setting age 30 as the end of early adulthood would however result in attributing senescent
68 deaths before age 30 (area *A1*) to the hump and ignoring deaths after age 30 that belong to the hump
69 component (area *A2*). Ignoring the heterogeneity of mortality phases or components overlooks the
70 possibility that, especially in young adult ages, a given death could be due to any of these forces.

71 The method we propose combines two common tools of demographic analysis: competing hazard
72 models and cause-deletion. We combine these approaches by deleting each cause of death and observing
73 the change in the shape components, which can be interpreted as the contribution of each cause
74 to each component. A similar idea was used in the past to split cause-of-death contributions into
75 ontogenescence and senescence (Gage, 1991), but this approach used the parametric model of Siler
76 (1979), which not only omits the hump, but also suffers from a lack of flexibility, like all parametric
77 models. This is why we use a non-parametric approach in all steps of our method. To preserve
78 coherence between all-cause mortality and cause-specific partitions, the estimation of cause-specific
79 contributions is simultaneous and constrained.

80 To simplify fitting, we work with mortality rates truncated at the age of observed minimum mor-
81 tality (near age 10) and 90, which are overwhelmingly attributable to the hump and senescence. Since
82 components are estimated non-parametrically, the senescence component is capable of accommodating
83 a plateau in very old ages if appropriate. Therefore, only hump and senescent components are fit
84 between ages 10 and 90. Formally, the method consists in three steps:

- 85 1. Reduce the set of causes of death to just those that are candidates to contribute to the young
86 adult hump.
- 87 2. Estimate the senescent and hump components of all-cause mortality.
- 88 3. Re-estimate both components on cause-deleted datasets, interpreting reductions in the hump
89 component as cause-specific contributions to the hump.

90 The first two steps are essentially applications of existing techniques, while the innovation rests in
91 the last step. In the next pages, each step is illustrated with the same toy example (Figure 2), which,
92 for ease of presentation, only contains three causes of death : A, B and C. Cause A displays a strong
93 hump between about age 15 and 40, and then decreases to a very low intensity. Cause B does not
94 display any hump, and it follows a Gompertz trend from age 10 onward. Cause B is at a high level
95 that makes it the leading cause of death after age 35, and even places it above cause A at the peak of
96 the hump. Cause C combines the characteristics of the previous two, making it the leading cause of
97 death between 16 and 35 years of age, dropping afterwards below cause B.

98 [Figure 2 about here.]

99 In terms of absolute mortality levels (e.g. death counts or life expectancy lost), if we define early
100 adulthood as 10 to 34, the causes of death rank as follows: $C > B > A$. It seems however that the

101 contributions of these causes to the deviation in the force of mortality (the hump) are in fact quite far
 102 from this. In particular, it is obvious from the shape of the age- and cause-specific death rates that
 103 cause B does not contribute at all to the deviation in the force of mortality, since it itself does not
 104 display any form of deviation around these ages. The method that we propose takes into account the
 105 contribution to the *deviation* of the force of mortality, rather than its absolute level.

106 2.1 Identify contributing causes of death

107 The first step in the decomposition of cause- and age-specific contributions to the young adult mortality
 108 hump is to identify the causes that are candidates to contribute to the hump. This step facilitates both
 109 the estimation and the interpretation of results. This selection can be based on theoretical arguments
 110 or, alternatively, follow a more inductive approach. The latter is especially useful in the case of many
 111 cause-of-death categories, where potential candidates could easily be overseen if cause-selection were
 112 entirely subjective.

113 In our example application we use Principle Components Analysis to identify the set of causes
 114 that are candidates to contribute to the hump, but other techniques can be used to identify the best
 115 candidates (See Section 3.2). In general, such data-driven techniques allow an exhaustive exploration
 116 of datasets containing large numbers of causes of death. In practice though, manual rearranging of the
 117 cause-of-death typology is often advisable. Including too many causes often results in some contribu-
 118 tions being too small to be estimated, and this causes convergence issues in fitting the decomposition
 119 model. Selecting too few causes limits the depth of the analysis.

120 2.2 Estimate all-cause components

121 The second step of the method consists in estimating additive shape components on the all-cause force
 122 of mortality. This can be done by fitting multiple-component models, sometimes known as competing
 123 hazard models (Gage, 1993), which decompose the force of mortality into additive components that
 124 reflect specific patterns in different age ranges. Historically, these models have often been defined by
 125 parametric functions, like those proposed by Thiele (1871), Heligman and Pollard (1980), Mode and
 126 Busby (1982) or Kostaki (1992), to cite only some that include a young adult mortality hump. Para-
 127 metric models are however limited because they fail to adapt to the diversity of mortality schedules,
 128 and they have been criticized for the high correlation between their parameters (Sharrow, 2011). The
 129 lack of flexibility is particularly crucial when dealing with cause-specific and cause-deleted mortality
 130 patterns, which cannot be easily described by fixed mathematical laws. These limitations motivated
 131 the development of a non-parametric alternative based on P -splines, called the Sum of Smooth Expo-
 132 nentials (SSE) model (Camarda, Eilers, & Gampe, 2016).

133 The SSE model, in its original mortality application, describes the force of mortality over age as
 134 the sum of three components similar in their interpretations to the ones defined by Heligman and
 135 Pollard (1980). In our case, we limit the ages to 10 to 90 and only fit two of these components, for
 136 the hump and senescence. This means that the force of mortality, $\boldsymbol{\mu}$, is modeled as the sum of two
 137 vectors $\boldsymbol{\gamma} = [\boldsymbol{\gamma}_H : \boldsymbol{\gamma}_S]$ over m ages. The subscripts denote which mortality component each $\boldsymbol{\gamma}_j$ refers
 138 to: Hump and Senescence, respectively. The model assumes that observed deaths \boldsymbol{d} are realizations
 139 from a Poisson distribution with a composed mean:

$$\boldsymbol{d} \sim \mathcal{P}(\boldsymbol{e}\boldsymbol{\mu} = \boldsymbol{C}\boldsymbol{\gamma}), \quad (1)$$

140 where \boldsymbol{e} is the population under exposure, and \boldsymbol{C} is given by

$$\boldsymbol{C} = \mathbf{1}_{1,2} \otimes \text{diag}(\boldsymbol{e}), \quad (2)$$

141 where $\mathbf{1}_{1,2}$ is a 1×2 matrix of ones, $\text{diag}(\boldsymbol{e})$ is the diagonal matrix of the exposure population and
 142 \otimes denotes the Kronecker product.

143 In this way, the composite matrix \boldsymbol{C} is an $m \times 2m$ matrix containing the population exposures in
 144 duplicate. The role of \boldsymbol{C} is to multiply each component by the exposures and simultaneously sum them
 145 up to obtain the expected values in (1). The model thus takes the form of a Composite Link Model

146 (Thompson & Baker, 1981) and is estimated with a penalized re-weighted least squares algorithm
 147 (Eilers, 2007).

148 Unlike parametric models, in the *SSE* model there is no need to make strong assumptions about
 149 the functional form of each component. For each component we assume a discrete sequence and we
 150 apply the exponential function to ensure non-negative elements:

$$\gamma_j = \exp(\mathbf{X}_j \boldsymbol{\beta}_j), \quad j \in \{H, S\}. \quad (3)$$

151 In other words, each component is described by a linear combination of a model matrix \mathbf{X}_j and
 152 associated coefficients $\boldsymbol{\beta}_j$. The design matrices \mathbf{X}_j can represent parametric or, in our case, non-
 153 parametric structures such as equally-spaced *B*-splines. In this way, the composite force of mortality
 154 $\boldsymbol{\mu}$ can be viewed as a sum of 2 exponential components, which potentially can be smooth. Further,
 155 the *SSE* model allows us to incorporate shape constraints to enforce senescence and young-adult
 156 components to be monotonically increasing and log-concave, respectively. These constraints ensure
 157 the identifiability of the model by ensuring that the two components are not interchangeable.

158 By fitting an *SSE* model to the overall force of mortality (Figure 3, black lines), we distinguish
 159 the expected deaths due to hump mortality ($\hat{\mathbf{d}}_H = \mathbf{e} \hat{\gamma}_H$) from those due to senescence ($\hat{\mathbf{d}}_S = \mathbf{e} \hat{\gamma}_S$).
 160 This additive construction acknowledges the fact that deaths that occur during early adulthood are
 161 not only specific to this phase of the life course, but also partly to the prevailing pattern of senescence.

162 2.3 Cause-of-death decomposition

163 Building on the *SSE* model, we propose a constrained approach to decompose the estimated hump
 164 into cause- and age-specific contributions ($\boldsymbol{\delta}_1^\kappa$). The cause-specific contributions can be defined as the
 165 difference between a given component estimated on the all-cause mortality and the same component
 166 estimated on cause-deleted data, where these specific causes were identified in the first step: $\boldsymbol{\delta}_j^\kappa =$
 167 $\gamma_j - \gamma_j^{-\kappa}$, where κ indicates the cause of death.

168 Both $\boldsymbol{\delta}_H^\kappa$ and $\boldsymbol{\delta}_S^\kappa$ for each of the two components (γ_H and γ_S) are estimated by refitting simulta-
 169 neously the *SSE* model on cause-deleted data. In our simulated example, this step only involves two
 170 causes: A and C. This constrained model can then be written as a system of constrained *SSE* models
 171 such as

$$\begin{cases} \mathbf{d}^{-A} \sim \mathcal{P}(\mathbf{C} \boldsymbol{\gamma}^{-A}) \\ \mathbf{d}^{-C} \sim \mathcal{P}(\mathbf{C} \boldsymbol{\gamma}^{-C}) \end{cases} \quad \text{subject to} \quad \begin{cases} \hat{\mathbf{d}}_H = \mathbf{e} \cdot (\boldsymbol{\delta}_H^A + \boldsymbol{\delta}_H^C) \\ \hat{\mathbf{d}}_S - \mathbf{d}^B = \mathbf{e} \cdot (\boldsymbol{\delta}_S^A + \boldsymbol{\delta}_S^C) \end{cases}. \quad (4)$$

172 The first two expressions define the two components ($\boldsymbol{\gamma}^{-\kappa}$) of the *SSE* model on the cause-deleted
 173 death counts ($\mathbf{d}^{-\kappa}$). The constraints in the last two equations ensure that cause-specific contributions
 174 sum up to the all-cause hump and senescence mortality components, respectively. Note that actual
 175 deaths by cause B, which does not present young adult excess mortality, are subtracted from the overall
 176 estimated senescent deaths to ensure that senescence components from causes A and C are coherently
 177 estimated.

178 Instead of achieving this optimization subject to equality constraints by Lagrange multipliers, we
 179 employ a simpler but accurate strategy. We incorporate our constraints in the system of equations
 180 and simultaneously estimate and constrain our outcomes.

To do so, we re-write the constraints in (4) as functions of the unknowns in the associated system
 of equations, i.e. $\boldsymbol{\gamma}^{-A} = [\boldsymbol{\gamma}_H^{-A} : \boldsymbol{\gamma}_S^{-A}]$ and $\boldsymbol{\gamma}^{-C} = [\boldsymbol{\gamma}_H^{-C} : \boldsymbol{\gamma}_S^{-C}]$:

$$\begin{aligned} \hat{\mathbf{d}}_H &= \mathbf{e} (\hat{\gamma}_H - \boldsymbol{\gamma}_H^{-A} + \hat{\gamma}_H - \boldsymbol{\gamma}_H^{-C}) & \hat{\mathbf{d}}_S - \mathbf{d}^B &= \mathbf{e} (\hat{\gamma}_S - \boldsymbol{\gamma}_S^{-A} + \hat{\gamma}_S - \boldsymbol{\gamma}_S^{-C}) \\ &= 2\mathbf{e} \hat{\gamma}_H - \mathbf{e} (\boldsymbol{\gamma}_H^{-A} + \boldsymbol{\gamma}_H^{-C}) & &= 2\mathbf{e} \hat{\gamma}_S - \mathbf{e} (\boldsymbol{\gamma}_S^{-A} + \boldsymbol{\gamma}_S^{-C}) \\ &= 2\hat{\mathbf{d}}_H - \mathbf{e} (\boldsymbol{\gamma}_H^{-A} + \boldsymbol{\gamma}_H^{-C}) & &= 2\hat{\mathbf{d}}_S - \mathbf{e} (\boldsymbol{\gamma}_S^{-A} + \boldsymbol{\gamma}_S^{-C}) \\ &= \mathbf{e} (\boldsymbol{\gamma}_H^{-A} + \boldsymbol{\gamma}_H^{-C}) & \hat{\mathbf{d}}_S + \mathbf{d}^B &= \mathbf{e} (\boldsymbol{\gamma}_S^{-A} + \boldsymbol{\gamma}_S^{-C}) \end{aligned}$$

181 In this way we can unify both system of equations and constraints in (4) in a single framework.
 182 Let $\check{\mathbf{d}}$ and $\check{\boldsymbol{\gamma}}$ denote the following vectors:

$$\begin{aligned} \check{\mathbf{d}} &= [\mathbf{d}^{-A} : \mathbf{d}^{-C} : \hat{\mathbf{d}}_1 : \hat{\mathbf{d}}_2 + \mathbf{d}^B] \\ \check{\boldsymbol{\gamma}} &= [\boldsymbol{\gamma}_1^{-A} : \boldsymbol{\gamma}_1^{-C} : \boldsymbol{\gamma}_2^{-A} : \boldsymbol{\gamma}_2^{-C}] \end{aligned} \quad (5)$$

183 The proposed approach becomes a single model with a composed mean as in (1):

$$\check{\mathbf{d}} \sim \mathcal{P}(\check{\mathbf{C}} \check{\boldsymbol{\gamma}}), \quad (6)$$

184 where the composite matrix takes the following form:

$$\check{\mathbf{C}} = \begin{bmatrix} \mathbf{I}_2 & \otimes & \mathbf{C} \\ \mathbf{1}_{1,2} & \otimes & \text{diag}(\mathbf{e} : \mathbf{e}) \end{bmatrix} \quad (7)$$

185 where \mathbf{I}_2 is an identity matrix of dimension 2, i.e. the number of components, and $\mathbf{1}_{1,2}$ is a matrix
186 of ones of dimension (1×2) , i.e. the number of hump-related causes.

187 In this way, by augmenting both \mathbf{C} to $\check{\mathbf{C}}$ and $\boldsymbol{\gamma}$ to $\check{\boldsymbol{\gamma}}$, we can still write the model as a Composite Link
188 Model. This allows us to estimate our complex decomposition by reliable algorithms and conveniently
189 include regression weights to strictly obey equality constraints in (4). Specifically, we assign in the
190 estimation procedure much larger weights to equations involving $\hat{\mathbf{d}}_1$ and $\hat{\mathbf{d}}_2 + \mathbf{d}^B$. A series of weights
191 equal to 10^5 works well in our case.

192 This whole procedure allows us to simultaneously estimate cause-specific contributions to each
193 component, constrained to sum to the overall components. As we demonstrate in Section 3, more hump-
194 related causes can be incorporated by a small augmentation of the model elements. An implementation
195 of these methods is available in an R package on the CRAN repository.

196 [Figure 3 about here.]

197 Figure 3 illustrates the application of this technique to our toy example. The black dots represent
198 all-cause age-specific death rates, and the black dashed lines represent the estimated hump and senes-
199 cence components. Each graph shows how these components are affected by the deletion of cause A
200 and C respectively, and the shaded area illustrates the contribution to the total hump from each cause
201 (δ_H^k). This figure also helps to characterize the respective contributions of each cause to the shape and
202 size of the hump: (1) The deletion of cause A only affects the hump component and not the senescence
203 component, while the deletion of cause C affects both; (2) the drop in the hump is larger after deletion
204 of cause C, which indicates a larger contribution of this cause to the hump; (3) the decrease in the
205 hump is larger before the peak in cause A, and after the peak in cause C, which means that their
206 contributions are not centered on the same age.

207 These characteristics can be better estimated by designing summary measures of the cause-specific
208 contributions to the hump. By working in a smooth setting, we are able to evaluate the components
209 with fine age-granularity. This allows us to consider components as continuous functions ($\delta_H^k(x) \approx \delta_H^k$).
210 These densities can be used to quantify the hump and its cause-specific contributions.

211 Although many dimensions of the hump can be studied, such as its height, location or spread, we
212 focus here on its general magnitude as measured by the potential gain in life expectancy that would re-
213 sult from the deletion of the cause-specific contribution to the hump. The total years of life expectancy
214 lost to the hump can be decomposed by age and cause using standard decomposition techniques (Ar-
215 riaga, 1984). This measure differs from what would be obtained with the direct application of these
216 standard methods because the contribution from the hump only represents a partial reduction of the
217 observed rates rather than a complete elimination of the observed rates in an age range .

218 In our example, the deletion of the overall hump would generate an increase of 0.73 years of
219 life expectancy, of which 0.18 years (24.7%) is due to cause A, and 0.54 years (75.3%) to cause C.
220 These proportions are very different from the gains in life expectancy induced by the total deletion of
221 deaths between ages 10 and 34 (1.86 years), of which causes A, B and C would contribute 0.23 years
222 (12.2%), 0.65 years (34.7%), and 0.99 years (53.1%) respectively. By taking into account the presence
223 of senescence at these ages and only considering the deaths in the young adult mortality hump, the
224 contribution of causes A and C to the hump is thus strongly reevaluated.

3 Application

3.1 Data

We use an early release of data produced by the Human Mortality Database (HMD, n.d.) on cause- and age-specific death rates for the USA between 1959 and 2010, covering ICD versions 7 through 10. These data are aggregated from National Center for Health Statistics deaths microdata into 92 cause categories. We first graduate the cause-specific death rates from abridged age groups to single ages using a cubic spline and then constrain to sum to single-age all-cause mortality rates from the Human Mortality Database. We make no adjustments to smooth potential coding ruptures, but none of the three ICD revisions (in 1968, 1979, and 1999) generates a visible rupture in the patterns we report (see Figure 6).

3.2 Cause-of-death selection

From the original 92 cause-of-death codes, we identify those that display a particular shape during early adulthood and are therefore good candidates to contribute to the hump. Since the causes that are the most susceptible to contribute to the hump are those that have the highest levels of change (both positive and negative) during young adulthood, we proceed by computing the first difference over age of the all-cause and each cause-specific force of mortality between ages 10 and 34. We then compute the Euclidean distance between each cause and all-cause mortality in order to get a general measure of how similar each cause's shape is to the overall mortality during the period of life affected by the hump. Repeating this analysis for each year yields 52 observations for each cause, which can be reduced to a few dimensions using Principal Component Analysis (PCA).

As indicated in Figure 4, the first two axes summarize over 95% of the information for both sexes. This means that the causes that stand out are generally the same over the whole period. The positions of causes on the first two dimensions highlight six causes that deviate from the rest: motor vehicle accidents, suicides, homicides, other accidents, "other" poisoning (i.e. non-alcoholic, mainly drug overdoses), HIV-AIDS, as well as maternal mortality for females. The pattern is clearer for males than for females, notably for non-traffic accidents, but we chose to use the same list for both sexes in order to ensure a direct comparison between sexes. We include maternal deaths in our typology because despite its similarity to the other causes between 10 and 34 it does stand apart at younger ages before converging with the other causes¹. This selection of causes is by no means canonical, but it is roughly coherent, and it accounts for the vast majority of the hump.

[Figure 4 about here.]

3.3 Results

3.3.1 Magnitude of the hump and comparison with standard decomposition methods

Most studies on young adult mortality use absolute age-specific death rates as the basis for measurement and comparison. To demonstrate the difference between our method and approaches based on absolute death rates, we first apply our decomposition method to separate the hump from the all-cause mortality rate schedule. The hump is itself a rate schedule, which can therefore be translated to years of life expectancy lost (LEL) (Arriaga, 1984). For comparison, we translate three total rate schedules to years of LEL: 1) the hump only, 2) all-cause absolute death rates between ages 10 and 34, and 3) just the undecomposed sum of the seven causes included in the hump between ages 10 and 34. The results of this exercise are shown in the top panel of Figure 5.

The LEL due to the seven selected causes is by definition smaller than that generated by all-cause mortality (Figures 5a and 5b). Most of the time, hump LEL is also lower than these seven causes because the senescent component has been removed. In some cases, such as in the early 1990s, a crossover is observed because the hump extends beyond the fixed age range used for the two

¹This is shown by the sensitivity analysis in Figure 4. A few other causes only stand apart after age 30 and are thus less likely to contribute to the hump.

270 comparisons (ages 10-34 in our case). The gap between all-cause and seven-cause LEL decreases over
271 time due to the decreasing share of other causes in deaths occurring between 10 and 34.

272 Although these three series share some similarities, such as an initial increase in the 1960s and
273 a sharp decrease in the late 1990s, trends differ in key ways. Specifically, trends in the hump and
274 all-cause (10-34) LEL are even of opposite sign. Between its maximum in 1969 and a local minimum
275 in 1983, the all-cause absolute LEL decreased by 20% for males and 27% for females, while the hump
276 impact increased by 6% for males and 68% for females. This means that during this period the decrease
277 in all-cause absolute LEL was due to changes in the senescence component, while the hump continued
278 to grow. We show later that this increase in the hump component comes from its widening rather than
279 an increase in intensity around its peak.

280 [Figure 5 about here.]

281 Figures 5c and 5d show the proportional cause-of-death contributions to LEL from all mortality
282 in ages 10 to 34. The proportional contribution of “other causes” decreases from 40% to 30% among
283 males and 60% to 50% for females over the whole period. This is consistent with the observation from
284 Figures 5a and 5b that the gap between the all-cause LEL and the 7-cause LEL declines over time.
285 The sudden compositional shift around 1987 is due to the introduction of HIV as a new cause-of-death
286 category

287 Figures 5e and 5f show the cause-of-death composition of the hump-only LEL for males and females.
288 Traffic and other accidents made up about 80% of the male hump-LEL in the 1960s. This situation
289 slowly evolved however over time, and nowadays these two causes only account for a third of the
290 hump-LEL. Meanwhile, suicides and homicides have grown from less than 10% to about half of the
291 male hump-LEL. Poisonings generally did not contribute more than 5%, except between 2000 and 2010
292 when the share grew to 17%. The story for males is thus very much about suicides and homicides
293 slowly replacing traffic accidents in the composition of the hump. The pattern is completely different
294 for females, as most of the hump-LEL can be explained by traffic accidents, with momentary increases
295 from homicides, other accidents and poisonings.

296 There are important compositional differences between causes in the hump-only (Figures 5e and
297 5f) versus the cause-specific LEL based on absolute rates (Figures 5c and 5d). The relative importance
298 of HIV to hump-LEL was for instance much higher than absolute death rates would suggest. The
299 portion of years of hump-LEL produced by traffic accidents is also in all years higher than that of
300 absolute traffic accident death rates. Moreover, the impact of homicides is stronger on the hump than
301 on absolute rates. The ranking of causes contributing to LEL is also different when we separate the
302 hump versus absolute death rates in ages 10-34, even ignoring “other causes”. On average, the mean
303 number of differences in ranking among causes between the two methods is 2.15 for males and 3.4 for
304 females. There are even years for which none (1992 and 1995 for males) or only one (2001 and 2004
305 to 2007 for females) of the seven causes occupies the same rank in both methods.

306 3.3.2 Shape of the hump by cause, over age, time, and cohorts

307 Results on the magnitude of the hump omit the shape of cause-of-death contributions to the hump.
308 We visualize patterns in rate-scale by plotting values over age and time in Lexis surfaces. Figure 6
309 shows surfaces of raw (undecomposed) cause-of-death rates. Visually, the all-cause surface does not
310 reveal any hump because all rates for young ages are dwarfed by the levels reached in old age due to the
311 senescence component. This is also the case for non-traffic accidents, which have a strong senescence
312 component. All other causes of death that were identified as potential contributors to the hump
313 display relatively high mortality during early adulthood. Some however combine this with other age
314 patterns, such as traffic accidents, which presents a bimodal shape with high mortality levels during
315 early adulthood as well as old age, or suicides, which also strongly affect older males and middle-
316 aged females. Homicides present even a tri-modal distribution, with highest rates observed among
317 infants, young adults, and in old ages. This picture of raw rates confirms that the causes of death
318 that contribute to the hump often also contribute to senescence or ontogenescence. Without a sharp
319 decomposition, considering all deaths from these seven causes as relating to the young adult mortality
320 hump would be an over-generalization.

321

[Figure 6 about here.]

322

[Figure 7 about here.]

323

324

325

326

327

328

329

330

331

332

We apply our model to the mortality of US males and females from 1959 to 2010 using the same set of causes of death. The cause and age-specific contributions are presented in the form of Lexis surfaces (Figure 7). In these surfaces the hump is now clearly visible, having been separated from the senescence component. The all-cause hump is neither stable in intensity nor age range over time (Figures 7a and 7h). From the beginning of our study period until the 1980s for males and 1970s for females, the hump is relatively compact and centered on age 20. The male hump in general is higher and wider than the female hump. Maximum age-specific hump contributions for males come from around age 20 in the 1970s, and for females around age 20 in 1980. The hump then widens progressively into the 30s and 40s, until approximately 1997 when it suddenly shrinks. Since the year 2000 the hump has resumed this process of widening into the 30s for both males and females.

333

334

335

336

337

338

339

340

341

342

These peculiarities in all-cause hump patterns are the sum of contributions from different causes of death, and so the primary contours in the all-cause hump are best explained in terms of its cause components. It is convenient to describe patterns in the contributions of each cause of death in terms of age, period and cohort patterns. Age patterns here refer to sudden increases or decreases in a contribution to the hump in a narrow age range over a wide range of years, and these are visible in the form of horizontal contours in the surfaces. Period patterns refer to a simultaneous changes in contributions to the hump over a broad range of ages, producing vertical contours in the surfaces. Cohort patterns here refer to differences in contributions to the hump between adjacent birth cohorts, producing contours running in 45° diagonal lines. Each of these patterns is clearly visible in at least some the causes contributing to the hump.

343

344

345

346

347

348

349

Age patterns are to some extent visible in each cause of death contributing to the hump. In the all-cause hump, this age effect manifests itself with a rapid increase hump mortality between ages 15 and 20, and a narrow peak between ages 20 and 25. The age patterns in increase and the peak are found in each of the hump causes of death except poisoning for males (Figure 7e). For HIV-AIDS onset follows a similar age pattern, but onset happens later around age 25 (Figures 7g and 7n). Patterns in the decline of the hump in higher ages are far less regular over time and causes of death, and show few clear horizontal contours, except perhaps traffic accidents among males (Figure 7b).

350

351

352

353

354

355

356

357

358

Period patterns in cause contributions to the hump are associated with the emergence of new threats that hit young adults particularly hard, or with new technologies or policies that simultaneously reduce risk over a range of young adult ages. The all-cause hump shows a strong period pattern in the form of a sudden decrease for both males and females around 1997. This pattern is mostly accounted for by HIV-AIDS for males (Figure 7g), but coincides with simultaneous drops in homicides for females (Figure 7k). A smaller period decrease is visible for males in the early 2000s, caused by simultaneous decreases in the hump contributions of suicides, homicides, and poisonings. Period increases are visible for HIV-AIDS for both males and females starting in the late 1980s (Figures 7g and 7n)², but also for female homicides in the early 1990s (Figure 7k).

359

360

361

362

363

364

Cohort patterns are primarily visible in the upper edge of the hump, i.e., in the way the hump fades into senescence. We see this pattern in male poisonings and suicides (Figures 7e and 7c), and female homicides (Figure 7k), each starting in cohorts born around 1950. Most cases of cohort hump effects in these results are paired with a constant age at onset, leading not only to an extension of the hump into higher ages, but to a general widening of the hump. Male poisonings (Figure 7e) are an exception to this, since this cause also displays a shift in age at onset.³

²The ICD code for HIV-AIDS was introduced in 1987, although this cause of death existed earlier. However, its spread was fast enough that it can be considered a period shock.

³When running the same decomposition in the cohort perspective, we see no such cohort pattern on the hump for poisoning among males born in the 1950s (only an excess around age 20), which suggests that this excess mortality is broadly specific to this cohort and not merely an attribute of its young adulthood. Figure 6e supports this speculation. In the period perspective, this produces an apparent cohort effect in the hump, which eventually dissolves into senescence.

3.4 Discussion of application to US data

Age patterns concern the age at onset, peak and fading of the hump into senescence. The former is relatively stable between 10 and 15 years of age, and applies to all causes of death except poisoning for males. This stability suggests that this dimension of the hump could be expressing a form of turmoil inherent to the nature of adolescence, as often conceived in the psychological literature (Freud, 1968; Hall, 1904). Recent studies show peculiar neurological developments in the adolescent brain⁴, which, according to some authors, generate a mismatch between the ability to anticipate and the regulation of emotions that could explain why adolescents more often engage in dangerous activities, particularly under peer-pressure (Casey, Jones, & Somerville, 2011; Steinberg, 2005).

The strong and regular patterns we observe in young adult excess mortality risk are consistent with these theories. That the peak in excess mortality occurs five or more years after these neurological changes may indicate a mortality lag between the acquisition of behaviors and mortality, due to either a phase of latency or the cushioning effect of age-related policies such as legal ages at driving or alcohol consumption. However, if an underlying biological process were a sufficient explanation for the hump, then we would only observe age patterns. Such regularity is apparent only in onset and peak for most (but not all) hump causes. We see irregularity in the location of the tail end of the hump, as well as strong period and cohort patterns for some causes, which point to other non-biological mechanisms.

The shape of the hump is indeed marked by shocks, both positive and negative, that are specific to certain years or periods of time. A good example of this pattern is the drop in maternal mortality seen in the early 1960s in Figure 7o, reflecting a longer decreasing trend over all maternal ages due to the diffusion of antibiotics and improvements in obstetric surgery (Loudon, 2000).

Homicide contributions to the hump also display period patterns (Figures 7d and 7k). A first rapid increase took place in the late 1960s to early 1970s, which particularly concerned young adults (LaFree, 1999). A second peak came in the early 1990s, particularly affecting young, black and hispanic males, and quickly decreased after 1993 (Cook & Laub, 2002). Our results show that females experienced an effect in the mid 1990s over a wider age range, possibly due to the presence of an accompanying cohort effect, or possibly due to underlying patterns in the age and sex differences between victims and perpetrators. There is no consensus about the causes of this wave of violent criminality. Explanations often involve changes in social support and economic inequalities (Pratt & Godsey, 2003), changes in size and strategy of police forces, and changes in crack-cocaine markets (Cook & Laub, 2002; LaFree, 1999; Levitt, 2004).

The strongest example of such period effects is undoubtedly the rapid spread of HIV-AIDS, for which ICD codes only began to capture in 1987 (Figures 7g and 7n). This cause of death not only increased the intensity of the hump, but also contributed to its spread into higher ages— well into ages 30-40. It suddenly diminished in 1996 with the introduction of antiretroviral therapies, which both lowered the risk of death and postponed the age at death beyond the hump (Palmisano & Vella, 2011). This drop of HIV-AIDS deaths explains a portion of the strong period effect observed in the all-cause hump between 1995 and 1998, but not entirely as our results show additional drops for suicides among males (Figure 7c), as well as homicides for females (Figure 7k).

Both the male and female all-cause hump display a clear progressive widening, starting around 1960 and 1980 respectively, before abruptly narrowing in the late 1990s (Figures 7a and 7h). This could potentially be interpreted from a period point of view as a progressive extension of the period of young adult excess mortality, but the fact that this widening happens roughly at a regular pace of one year of age per calendar year suggests that this may be a cohort effect concerning people born around or after 1950. This means that this cohort experienced a higher mortality than earlier cohorts, and contributed to a widening of the hump by progressively increasing the tail age of the hump.

For suicides and homicides, an age effect is superposed on the cohort effect, generating a triangle pattern on the lexis surfaces (Figures 7c and 7d), but not for poisonings (Figure 7e). When the cohorts born between roughly 1945 and 1970 leave the age-range of the hump, their higher mortality for these specific causes is retained but blends into the general level of senescence. This pattern is accompanied by a genuine period decrease in these causes around 1997 (visible in Figures 6c and 6d), but could also

⁴These changes concern the dopaminergic activity due to the unsynchronized development of myelination and gray matter in prefrontal areas of the brain that control social cognition and anticipation, and of the limbic system, that controls emotions and feelings of reward (Giedd, 2004; Lenroot & Giedd, 2006; Steinberg, 2010).

416 explain some of the period patterns. For males, this cohort effect is obvious for suicide and poisonings,
417 and more subtle for homicides, from the 1960s to the 1990s. This predates the equivalent widening
418 observed on the all-cause hump by about a decade. The male hump appeared to spread later than the
419 female hump because it was initially broader, due to a wider contribution of traffic accidents, which
420 temporarily concealed cohort patterns in homicide, suicide, and poisonings that had begun in the 1960s
421 (Figures 7c, 7d and 7e).

422 These cohort observations confirm previous findings that mortality increased for the cohorts born
423 after 1945 for suicide (Chauvel, Leist, & Ponomarenko, 2016; Stockard & O'Brien, 2006), homicide
424 (O'Brien & Stockard, 2002, 2006), and poisoning (Miech, Koester, & Dorsey-Holliman, 2011), reaching
425 a peak with cohorts born in the 1960s. This cohort phenomenon has been given similar explanations
426 for each of these three causes of death, including a large relative cohort size (a so-called Easterlin-
427 effect), a higher percentage of non-marital births, higher exposure to drug use, and a lower degree of
428 social integration and regulation (O'Brien & Stockard, 2002, 2006; Stockard & O'Brien, 2006), as well
429 as the rise of socioeconomic stressors, particularly among non-Hispanic, low-educated, and unmarried
430 members (Chauvel et al., 2016).

431 The resemblance in the patterns of homicide, suicide, and poisoning is thus partly explained by
432 the fact that they share common underlying social dynamics. There is also a risk of misclassification
433 between all three causes, but particularly between suicide and poisoning. Qualitative studies suggest
434 that suicides may be classified as poisonings to a significant yet unmeasurable extent (Miech, Bohnert,
435 Heard, & Boardman, 2013, 138). Some of the similarities between the hump contributions from suicide
436 and poisoning may be due to this kind of coding imprecision, but we have no reason to suspect that
437 aggregate patterns are accounted for by coding peculiarities.

438 4 Conclusion

439 We conceive of the young adult mortality hump as excess mortality beyond the prevailing senescent
440 level of mortality. Research on young adult mortality should consider this difference when focusing
441 on this specific phase of the life course. We propose a method to flexibly measure the hump and
442 decompose it into its cause-of-death contributions. This method characterizes the hump not merely in
443 terms of peak location (Goldstein, 2011) or a restrictive set of parameters (Heligman & Pollard, 1980,
444 e.g.), but it estimates a full schedule of hump mortality rates by cause of death.

445 We apply this method to mortality rates by cause of death in the United States from 1959 to
446 2010 and offer a first look at trends in the hump in isolation from background mortality. When
447 isolated, trends in the U.S. hump differ qualitatively from trends in observed mortality rates in the
448 same age-range. Specifically, we document countervailing trends in the hump magnitude based on
449 decomposed versus observed rates. When broken down by cause of death, we also observe differences
450 in the magnitude, ranking, and trends in particular cause-of-death contributions to life expectancy lost
451 to the hump. The age of the peak of the hump has been relatively stable in the United States, but its
452 spread has undergone large and regular changes articulated along age, period, and cohort lines.

453 More specifically, the results show a progressive widening of the hump starting in the 1960s and
454 coming to an abrupt halt in the late 1990s. This pattern is due partly to the excess mortality of the
455 cohorts born after 1950 in suicides, homicides, and poisonings, as well as period shocks like the rise and
456 fall of the HIV-AIDS epidemic in the late 1980s and early 1990s. Males in the United States have a
457 larger hump than females, and underwent a continuous decrease in the contribution of traffic and other
458 accidents, which was offset by increases in contributions from suicides, homicides, and poisonings. The
459 female mortality hump was mainly driven by traffic accidents and homicides. For both males and
460 females, HIV-AIDS played a much more important role in the hump than it did in overall observed
461 mortality rates.

462 The application of our method to U.S. data reveals mortality patterns that otherwise remain
463 partially hidden from view and analysis. It is our hope that better measurement will lead to increased
464 understanding of the force of mortality in young adult ages, and the relationship between other changes
465 during young adulthood and aggregate mortality outcomes. Such applications could fruitfully target
466 specific subpopulations and contexts. Simultaneous estimation of the model over age and time would
467 help stabilize results for such specific analyses of smaller populations.

References

- 469 Andreev, E. (1982). Metod komponent v analize prodoljitelnosti zjizni. [the method of components
470 in the analysis of length of life]. *Vestnik Statistiki*, 9, 42-47.
- 471 Arriaga, E. E. (1984). Measuring and explaining the change in life expectancies. *Demography*, 21(1),
472 83-96.
- 473 Blum, R. W. (2009). Young people: not as healthy as they seem. *The Lancet*, 374(9693), 853-854.
- 474 Camarda, C. G., Eilers, P. H., & Gampe, J. (2016). Sums of smooth exponentials to decompose
475 complex series of counts. *Statistical Modelling*, 16(4), 279-296.
- 476 Casey, B., Jones, R. M., & Somerville, L. H. (2011). Braking and accelerating of the adolescent brain.
477 *Journal of Research on Adolescence*, 21(1), 21-33.
- 478 Chauvel, L., Leist, A. K., & Ponomarenko, V. (2016). Testing persistence of cohort effects in the
479 epidemiology of suicide: an age-period-cohort hysteresis model. *PLOS ONE*, 11(7), e0158538.
- 480 Cook, P. J., & Laub, J. H. (2002). After the epidemic: Recent trends in youth violence in the united
481 states. *Crime and Justice*, 29, 1-37.
- 482 Eilers, P. H. (2007). Ill-posed problems with counts, the composite link model and penalized likelihood.
483 *Statistical Modelling*, 7(3), 239-254.
- 484 Freud, A. (1968). Adolescence. In A. E. Winder & D. Angus (Eds.), *Adolescence : contemporary*
485 *studies* (2d ed. ed.). New York: American Book.
- 486 Gage, T. B. (1991). Causes of death and the components of mortality: Testing the biological inter-
487 pretations of a competing hazards model. *American Journal of Human Biology*, 3(3), 289-300.
- 488 Gage, T. B. (1993). The decline of mortality in england and wales 1861 to 1964: Decomposition by
489 cause of death and component of mortality. *Population Studies*, 47(1), 47-66.
- 490 Giedd, J. N. (2004). Structural magnetic resonance imaging of the adolescent brain. *Annals of the*
491 *New York Academy of Sciences*, 1021(1), 77-85.
- 492 Goldstein, J. (2011). A secular trend toward earlier male sexual maturity: Evidence from shifting ages
493 of male young adult mortality. *PLoS ONE*, 6(8).
- 494 Gompertz, B. (1825). On the nature of the function expressive of the law of human mortality, and
495 on a new mode of determining the value of life contingencies. *Philosophical Transactions of the*
496 *Royal Society of London*, 115, 513-583.
- 497 Hall, S. (1904). *Adolescence: Its psychology and its relations to physiology, anthropology, sociology,*
498 *sex, crime, religion and education*. New York: D. Appleton and company.
- 499 Heligman, L., & Pollard, J. H. (1980). The age pattern of mortality. *Journal of the Institute of*
500 *Actuaries*, 107.
- 501 Heuveline, P. (2002). An international comparison of adolescent and young adult mortality. *The*
502 *ANNALS of the American Academy of Political and Social Science*, 580(1), 172-200.
- 503 HMD. (n.d.). *Human mortality database. university of california, berkeley (usa), and max*
504 *planck institute for demographic research (germany). available at www.mortality.org or*
505 *www.humanmortality.de.*
- 506 Horiuchi, S., & Wilmoth, J. R. (1998). Deceleration in the age pattern of mortality at olderages.
507 *Demography*, 35(4), 391-412.
- 508 Kostaki, A. (1992). A nine-parameter version of the heligman-pollard formula. *Mathematical Popula-*
509 *tion Studies*, 3(4), 277-288.
- 510 LaFree, G. (1999). Declining violent crime rates in the 1990s: Predicting crime booms and busts.
511 *Annual Review of Sociology*, 25, 145-168.
- 512 Lenroot, R. K., & Giedd, J. N. (2006). Brain development in children and adolescents: Insights from
513 anatomical magnetic resonance imaging. *Neuroscience & Biobehavioral Reviews*, 30(6), 718-729.
- 514 Levitis, D. A. (2011). Before senescence: the evolutionary demography of ontogenesis. *Proceedings of*
515 *the Royal Society B: Biological Sciences*, 278(1707), 801-809.
- 516 Levitt, S. D. (2004). Understanding why crime fell in the 1990s: Four factors that explain the decline
517 and six that do not. *The Journal of Economic Perspectives*, 18(1), 163-190.
- 518 Loudon, I. (2000). Maternal mortality in the past and its relevance to developing countries today. *The*
519 *American Journal of Clinical Nutrition*, 72(1), 241s-246s.
- 520 Miech, R., Bohnert, A., Heard, K., & Boardman, J. (2013). Increasing use of nonmedical analgesics

- 521 among younger cohorts in the united states: A birth cohort effect. *Journal of Adolescent Health*,
522 52(1), 35-41.
- 523 Miech, R., Koester, S., & Dorsey-Holliman, B. (2011). Increasing us mortality due to accidental
524 poisoning: the role of the baby boom cohort. *Addiction*, 106(4), 806-815.
- 525 Mode, C., & Busby, R. (1982). An eight-parameter model of human mortality - the single decrement
526 case. *Bulletin of Mathematical Biology*, 44(5), 647-659.
- 527 O'Brien, R. M., & Stockard, J. (2002). Variations in age-specific homicide death rates: A cohort
528 explanation for changes in the age distribution of homicide deaths. *Social Science Research*,
529 31(1), 124-150.
- 530 O'Brien, R. M., & Stockard, J. (2006). A common explanation for the changing age distributions of
531 suicide and homicide in the united states, 1930 to 2000. *Social Forces*, 84(3), 1539-1557.
- 532 Palmisano, L., & Vella, S. (2011). A brief history of antiretroviral therapy of hiv infection: success
533 and challenges. *Annali dell'Istituto superiore di sanit f*, 47(1), 44-48.
- 534 Patton, G. C., Coffey, C., Sawyer, S. M., Viner, R. M., Haller, D. M., Bose, K., ... Mathers, C. D.
535 (2009). Global patterns of mortality in young people: a systematic analysis of population health
536 data. *The Lancet*, 374(9693), 881-892.
- 537 Pollard, J. H. (1982). The expectation of life and its relationship to mortality. *Journal of the Institute
538 of Actuaries*, 109(2), 225-240.
- 539 Pratt, T. C., & Godsey, T. W. (2003). Social support, inequality, and homicide: A cross-national test
540 of an integrated theoretical model. *Criminology*, 41(3), 611-644.
- 541 Pressat, R. (1985). Contribution des  carts de mortalit  par  ge   la diff rence des vies moyennes.
542 *Population*, 40(4/5), 766-770.
- 543 Sharrow, D. J. (2011). *Heligman pollard mortality model parameter estimation using bayesian melding
544 with incremental mixture importance sampling*.
- 545 Siler, W. (1979). A competing-risk model for animal mortality. *Ecology*, 60(4), 750-757.
- 546 Steinberg, L. (2005). Cognitive and affective development in adolescence. *Trends in Cognitive Sciences*,
547 9(2), 69-74.
- 548 Steinberg, L. (2010). A dual systems model of adolescent risk-taking. *Developmental psychobiology*,
549 52(3), 216-224.
- 550 Stockard, J., & O'Brien, R. M. (2006). Cohort variations in suicide rates among families of nations.
551 *International Journal of Comparative Sociology*, 47(1), 5-33.
- 552 Thiele, T. N. (1871). On a mathematical formula to express the rate of mortality throughout the
553 whole of life, tested by a series of observations made use of by the danish life insurance company
554 of 1871. *Journal of the Institute of Actuaries and Assurance Magazine*, 16(5), 313-329.
- 555 Thompson, R., & Baker, R. (1981). Composite link functions in generalized linear models. *Applied
556 Statistics*, 125-131.
- 557 Vaupel, J. W. (1997). Trajectories of mortality at advanced ages. *Between Zeus and the salmon: The
558 biodemography of longevity*, 17-37.

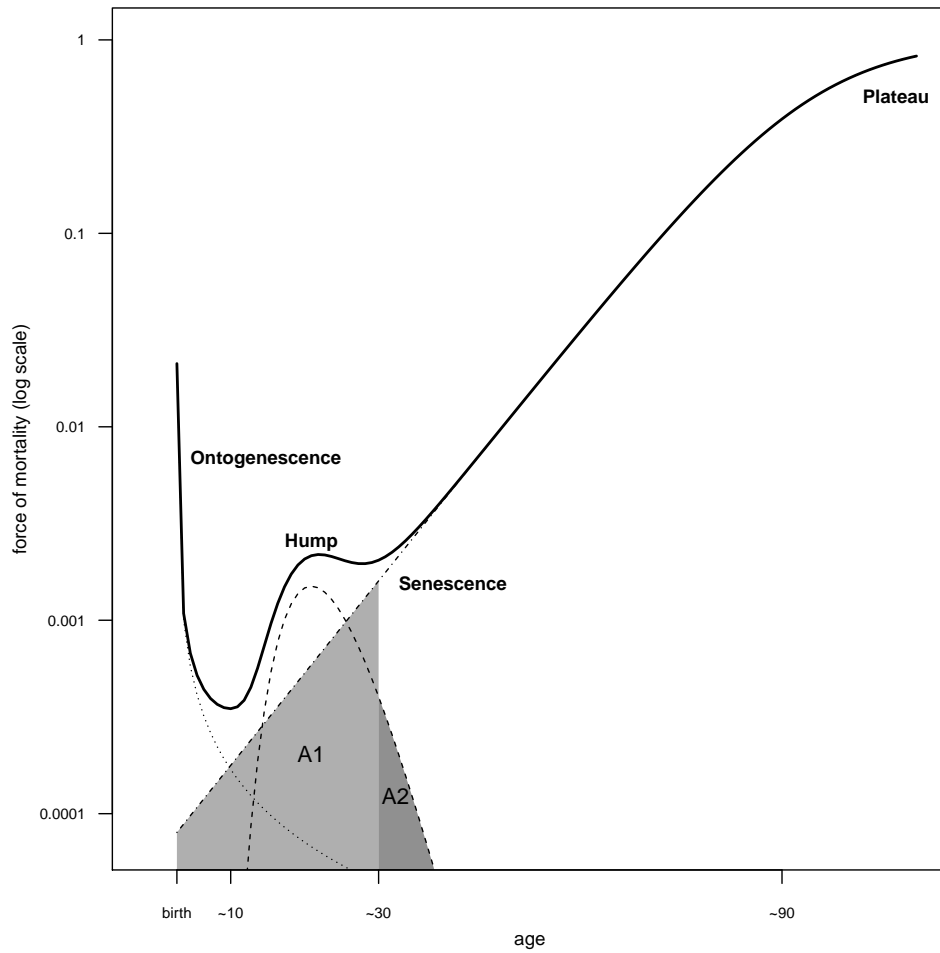


Figure 1: The total force of mortality over the life course is usually composed of three phases: a decreasing trend during the first decade of life, a hump in the second and third decade, and an increasing trend thereafter, marked by a progressive deceleration in very old age. This aggregated evolution does not necessarily reflect the experience of risk in individuals. Area *A1* represents senescent mortality between age 10 and 30, while area *A2* represents hump mortality after age 30.

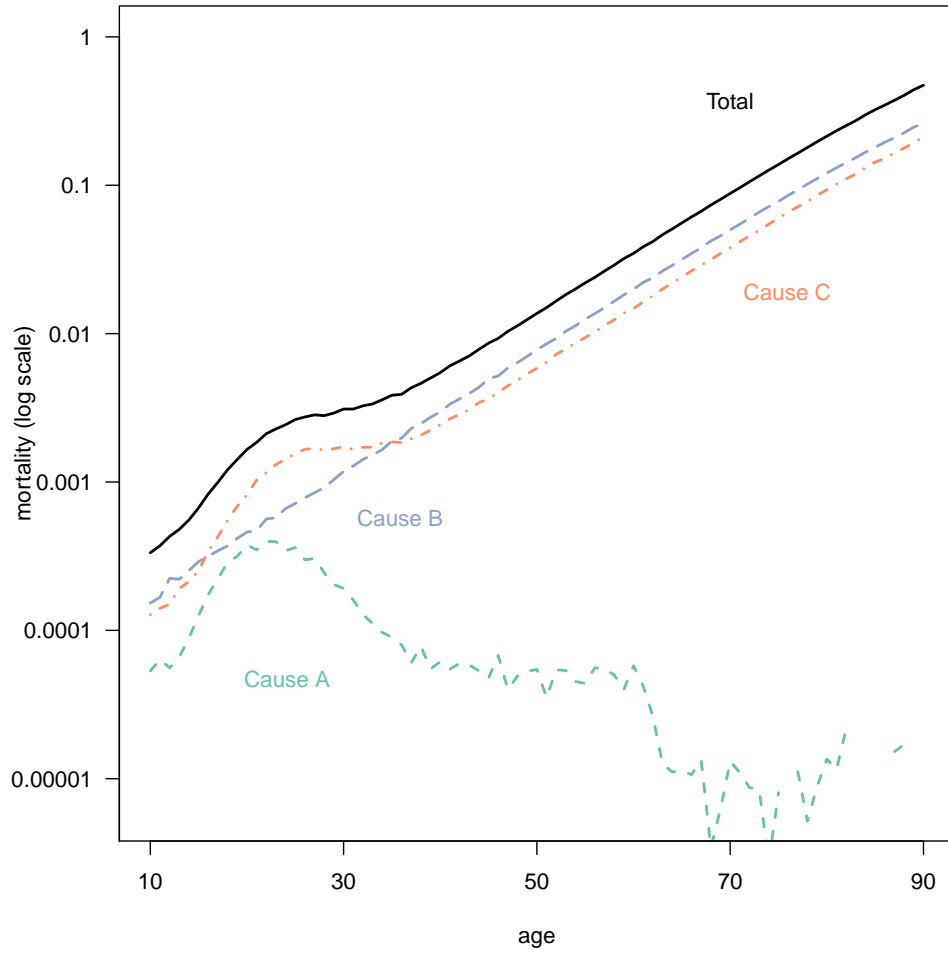


Figure 2: Cause- and age-specific death rates for simulated example. Causes A and C contribute to the hump. Causes B and C contribute to senescence.

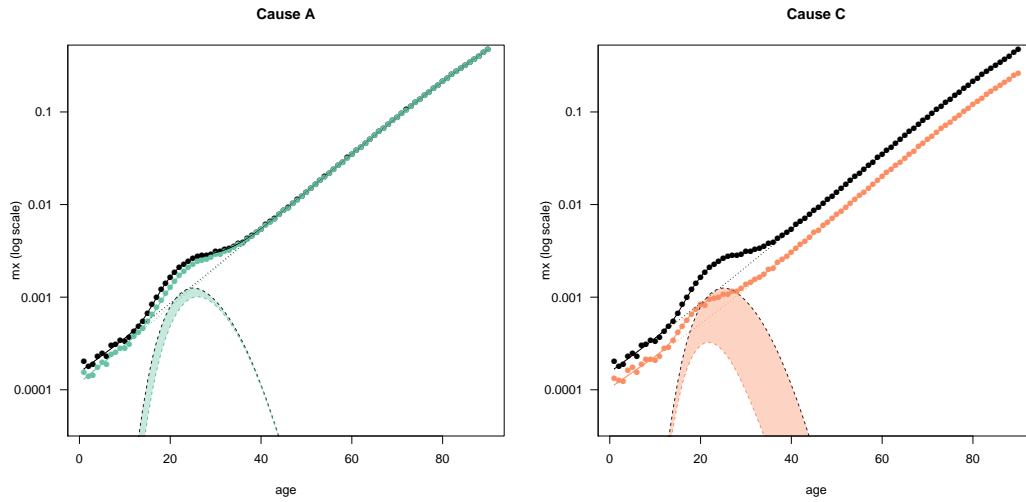


Figure 3: Cause-deleted mortality for simulated example. All-cause and cause-deleted mortality are plotted in black and colored dots respectively. The hump and senescence components are plotted in dashed lines. The difference between all-cause and cause-deleted hump components (shaded areas) represents the cause-specific contribution to the hump component.

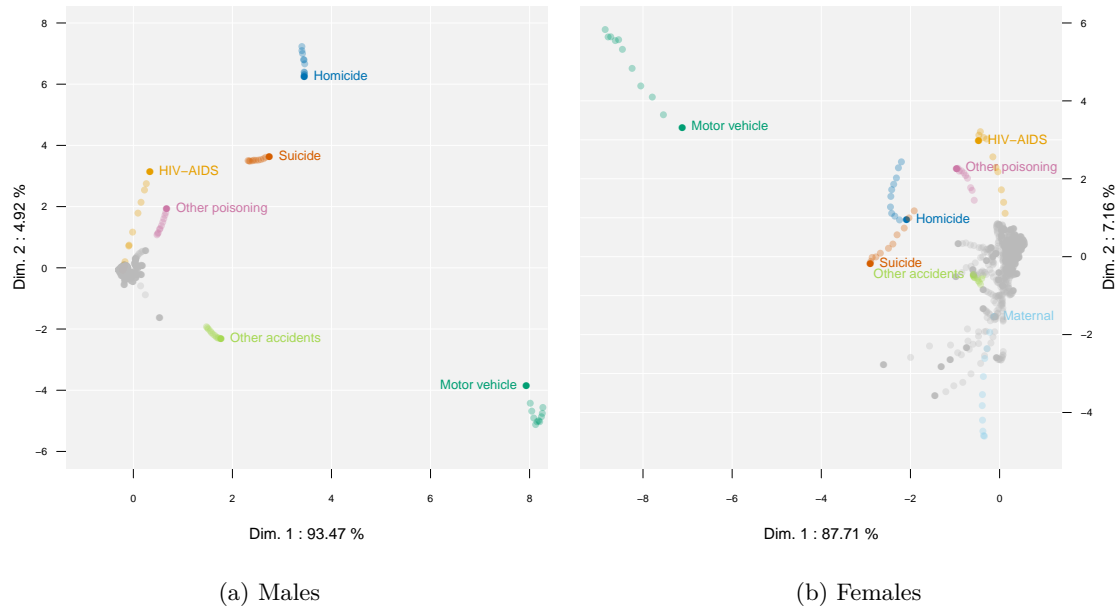


Figure 4: Difference in shape between each cause of death and all-cause mortality from 10 to 34 years of age. For each year from 1959 to 2010 we computed the first differences of the cause-specific forces of mortality and compared it with the all-cause equivalent using the Euclidean distance as a unique summary measure. The information from these 52 years is reduced by Principal Components Analysis (PCA) and represented on standardized scales. Seven causes of death are flagged for their unusual shape: traffic accidents, homicides, suicides, poisoning, HIV-AIDS, other accidents, and maternal mortality. Sensitivity analysis was performed by varying the end of the age range from 24 to 34, and plotting the results as supplementary observations on the PCA with lighter colors.

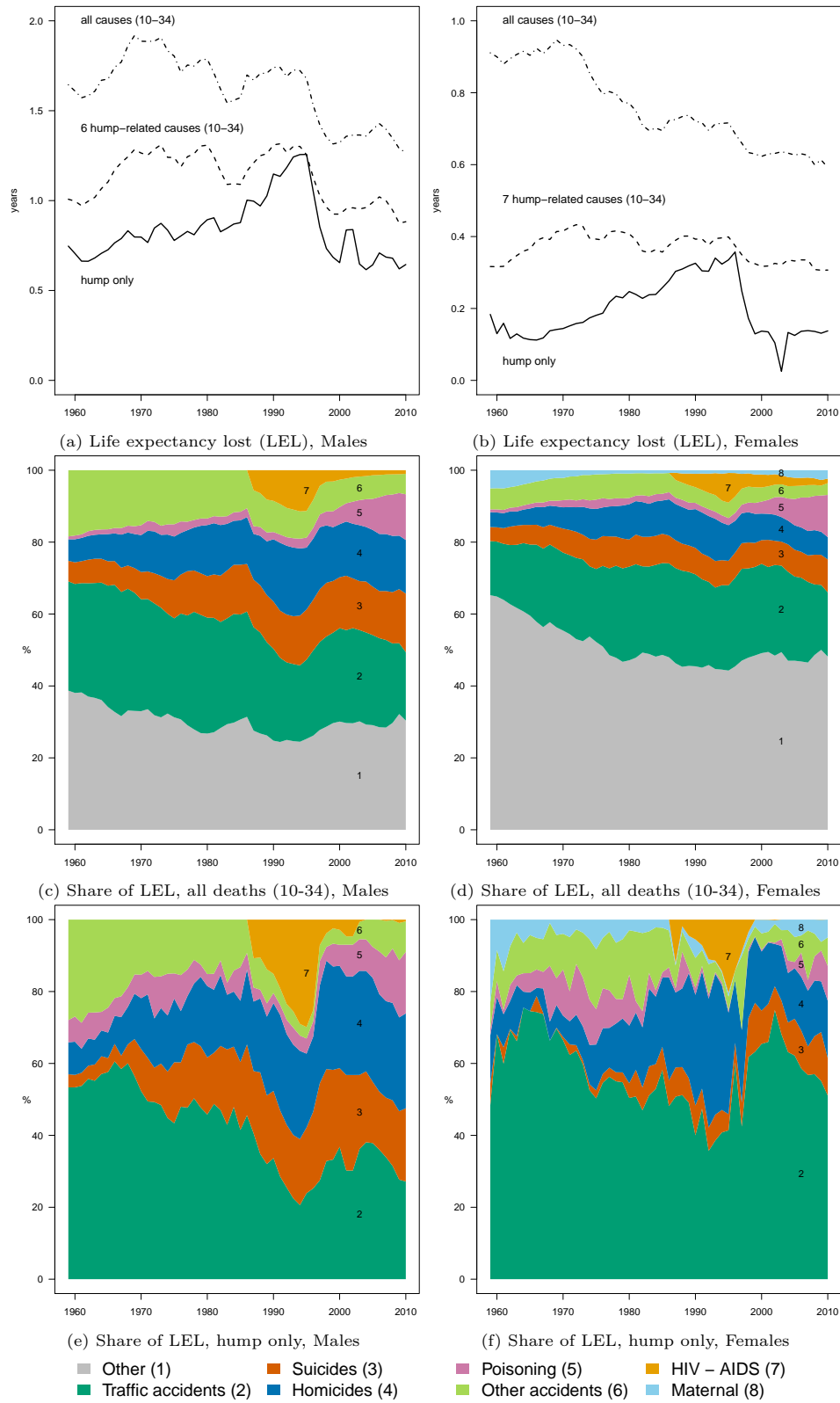


Figure 5: Application of our method to US mortality between 1959 to 2010. We compare a classical decomposition applied to ages 10 to 34, and our proposed method focusing on the hump only. Units are expressed in terms of the difference in years of life expectancy between the observed force of mortality and after deleting either all deaths, only those coming from the previously-identified seven causes linked with the hump, and only the contribution of these causes to the hump respectively.

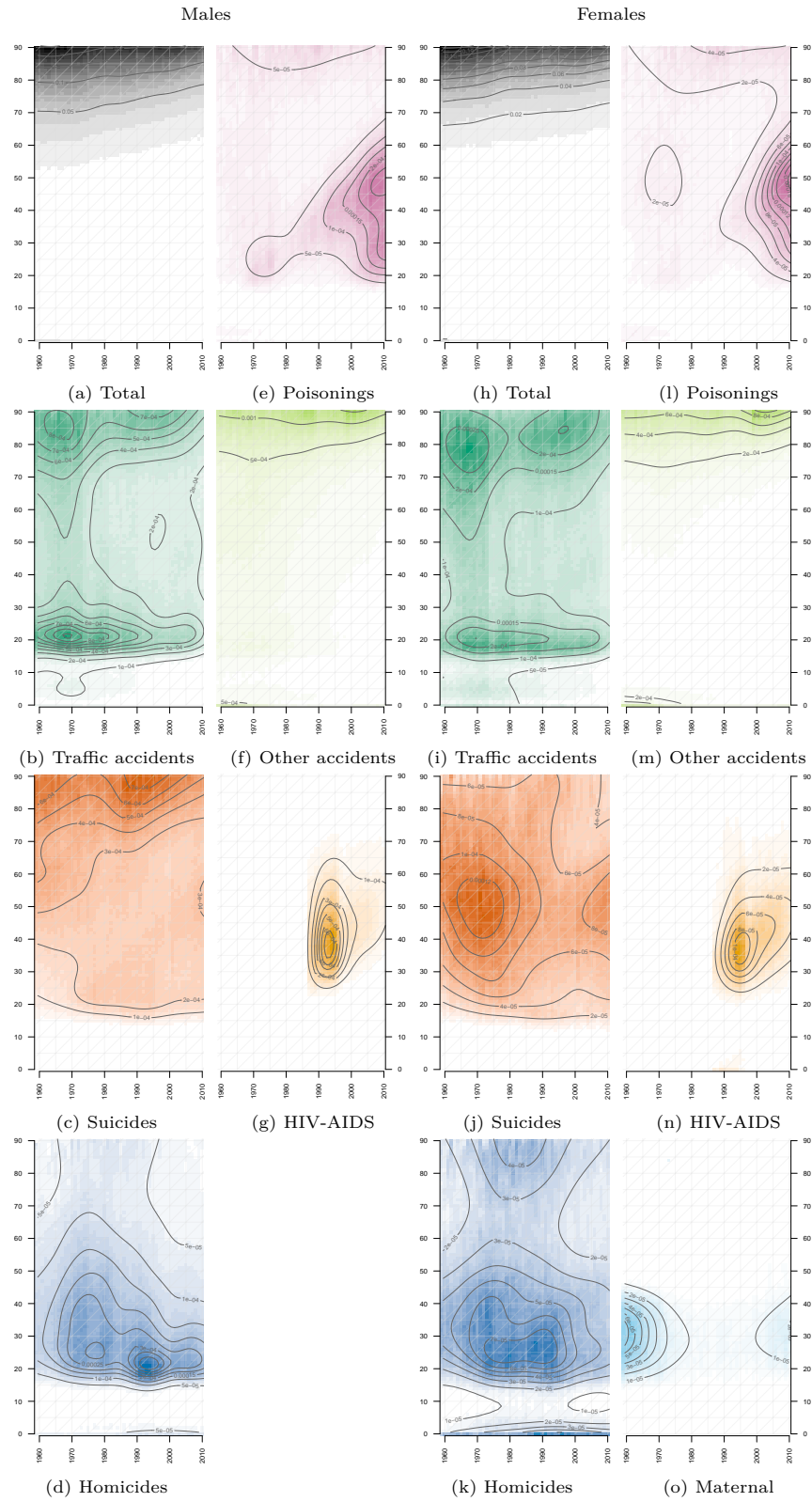


Figure 6: Lexis surfaces of cause-specific death rates, US males and females 1959-2010. Each cause is plotted on a dedicated color scale, and smoothed contours are superimposed to give an indication of the magnitude.

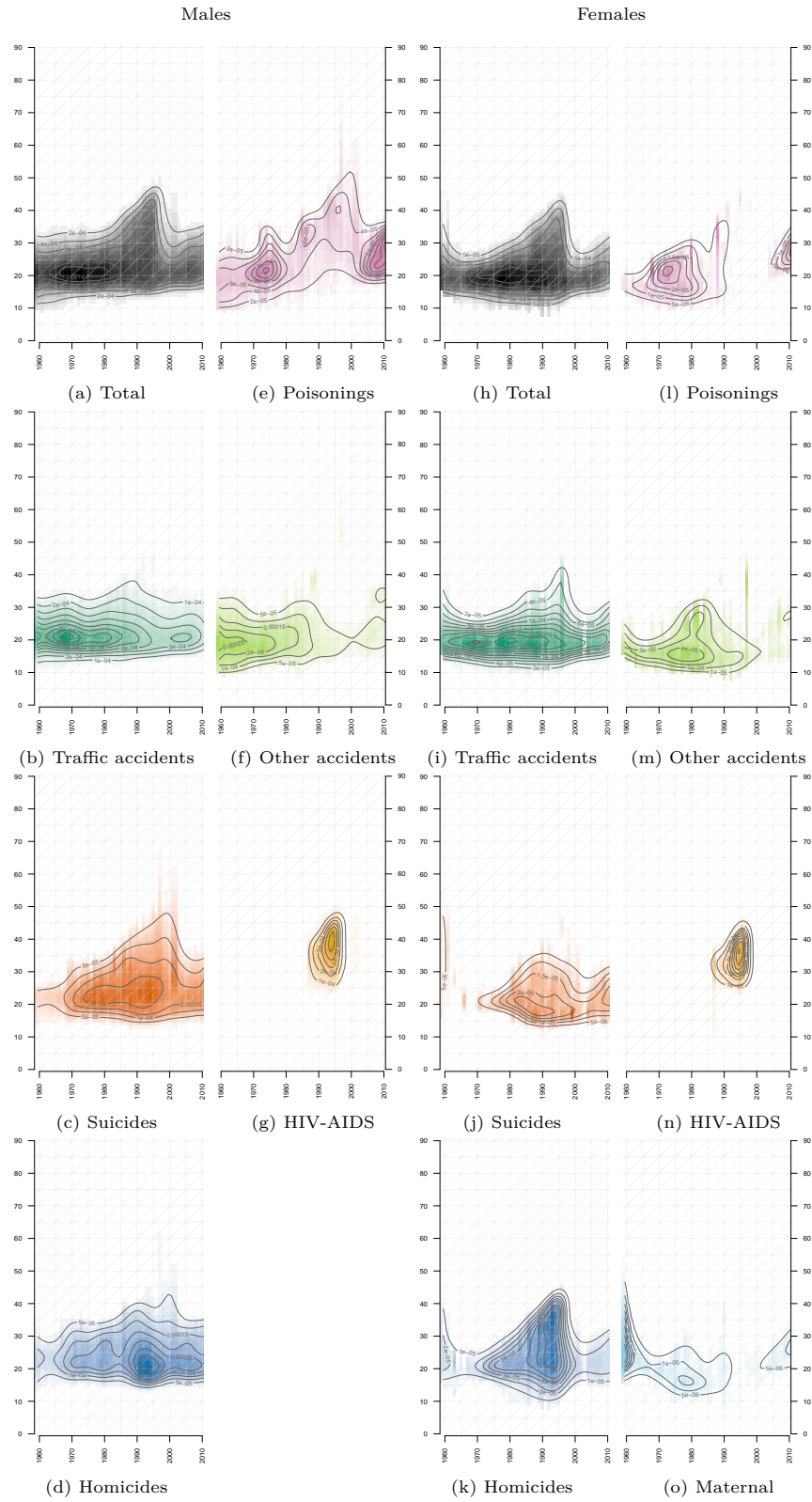


Figure 7: Lexis surfaces of cause-specific contributions to the hump, US males and females 1959-2010. These correspond to the $\delta_1^{\mathcal{K}}$ computed for each year. Each cause is plotted on a dedicated color scale, and smoothed contours are superimposed to give an indication of the magnitude.